Structural design and experimental verification of a novel split aileron wing

Anmin Zhao[1], Dongyu He[1], Dongsheng Wen[1,2*]

1. National key Laboratory of Human Machine and Environment Engineering, School of Aeronautical Science and Engineering, Beihang University, Beijing, 100191, China

2. School of Chemical and Process Engineering, University of Leeds, U.K

Abstract

To improve aerodynamic performance and attain a lighter weight of wing for use in small (<30 kg) drones, a novel design scheme of split aileron is proposed based on a similar application of the split flap, which enables the airplane to operate rolling movement. The function of the separated aileron is implemented utilizing an electro-servo system that is actuated through a brushless direct current motor (BLDCM). The design of three conceptual configurations of the clam-shell aileron structure, including the upper, middle, and bottom positions with deflection angle of 31^0 and 15^0 downwards, are studied numerically and theoretically. Based on the optimal design of the bottom position of the split aileron structure, the aerodynamic characteristics and structural weight of the separated aileron are evaluated by comparison with a traditional hinged aileron. The results indicate that the proposed design of the detached aileron can enhance the average aerodynamic efficiency of the wing by 16.3 % and reduce the weight of the wing by 49.5%. The functional prototype of the split aileron wing airplane is established and manufactured based on the proposed design. The flight test results confirm applicability of the clam-shell aileron to control the rolling motion of aircraft. The split aileron is potentially exploited for the fixed-wing unmanned aerial vehicles (UAVs) in practical engineering application.

Keywords: split aileron, aerodynamic performance, structural weight, function prototype,

flight test

1. Introduction

Acquiring a no-gap upper surface of the wing is one of the ideal goals in aviation design. To maximize the aerodynamic efficiency and decrease the structural weight of wing, blended wing body (BWB) technology [1-4] could be usually introduced, which is mainly for military unmanned aerial vehicles (UAVs) and high-speed aircraft. Indeed, the demands of smoothness surface and lighter weight for small and low speed (<50m/s) UAV lead designers to think out such a perfect plane, which has the ability to control the rolling motion of the aircraft without a traditional hinged aileron.

It is known that a configuration of the split flap can not only increase the camber of the wing which increases the lift introduced, but also attain a yaw-control of the airplane. Many verifications have been conducted to reveal above control features [5-8] in flight by numerical computation and theoretical analysis. To obtain a yaw motion of the airplane by the deflection of rudder on one side of the wing, a split drag flap was designed based on UiTM's BWB UAV Baseline-II E-4 by Firdaus Mohamad et al. [9], reporting that asymmetric drag force of the wing was generated, and yawing moment was produced. The effects of different airspeeds and angles of attack on directional control were investigated in wind tunnel by Gloria Stenfelt et al. [10], noting that a yaw moment was achieved through the split flap deflection on one wing. In addition, Nicolas Molin et al. [11].explored a two-element wing model with a split flap configuration impacted on noise control, it was discovered that the noise was dropped in mid frequency noise due to the shear layer was weakened when the flow crossed the gap. Clearly, the function of the controlling yaw motion and decreasing noise of the airplane could be

reached by the layout of the split flap. Thus, a thought was induced by the design scheme of the split flap, whether it is possible to design a split aileron that complies with the function of a conventional hinged aileron by deflection of a one-sided split aileron.

Moreover, the configuration of the flying-wing aircraft has received considerable attention. The idea of using the split drag rudder to control the yaw for tailless flying-wing aircraft has been proposed for a long time [12-14]. A mechanical feature of the split-drag-rudder was investigated by Zhongjian Li and Dongli Ma [15], who carefully analyzed its yawing control characteristics, three-axis control coupling effect, as well as influencing regularities on aerodynamics and stabilities, and to some extent, help to solve the yawing control problem for the flying wing configuration. Daochun Li et al. [16] examined a new morphing drag rudder based on the chord-wise continuous variable camber technology. The results show that the morphing drag rudder experiences a larger aerodynamic drag than the traditional one at small angles of attack. A configuration based on differential operation of split drag-rudders around a certain variable bias was presented by Jahanzeb Rajput [17] et al. and reveled that the control efficiency of split drag-rudders at low speed flight with large angle-of-attack could be improved. Wherein the aerodynamic performance of the split drag-rudders of flying wing airplane is sufficient to control the motion of the aircraft. Consequently, an idea was motivated by the design scheme of split drag-rudders, whether it is possible to design a split aileron structure with good aerodynamic performance to meet the requirements of flight control.

It is evidently that there are some extensive studies on the aerodynamic and structure of the split drag flaps wing in the open literature, the study relevant to the split aileron, however,

has not been reported. The propose of the current research to investigate a new configuration of a split aileron using the inspiration of the split flap design. The divided aileron that is located on the lower surface of the trailing edge of each wing for airplane and that separates from the wing structure when rotated downward, brings an increase in lift for airplane roll control. The results demonstrate that the proposed design of split aileron can enhance the average aerodynamic efficiency by 16.3 % and decrease structural weight of 52.2 g. The success of the flight test result reveals that the design scheme of the detached aileron is significant in practical engineering applications.

2. Conceptual of split aileron design

In this section, a creative design concept of the split aileron is proposed. The lateral motion of an aircraft can be commanded by the separated aileron that is actuated by an independent servosystem actuator of brushless DC (Direct Current) motor. Based on the design proposal of the clam-shell aileron, a complete smooth upper surface of the wing is achieved.

2.1 Split aileron design

A standard airfoil of Eppler 66 is chosen in Fig 1a, which has a max thickness 10.1% at 28.7% chord, max camber 4.1% at 52.3% chord and chord length of 304mm. As illustrated in Fig. 1b-1d, three configurations of separated aileron are designed by adjusting only the installation position of the calm-shell aileron without changing the geometry shape of the trailing edge of the wing. The angle of the split aileron is corresponding to 15 degrees in the left column, and an angle of 31 degrees is represented in the right column. The distance from the leading-edge of the wing to parallel to the axis of rotation is 197cm, 202cm, and 212cm,
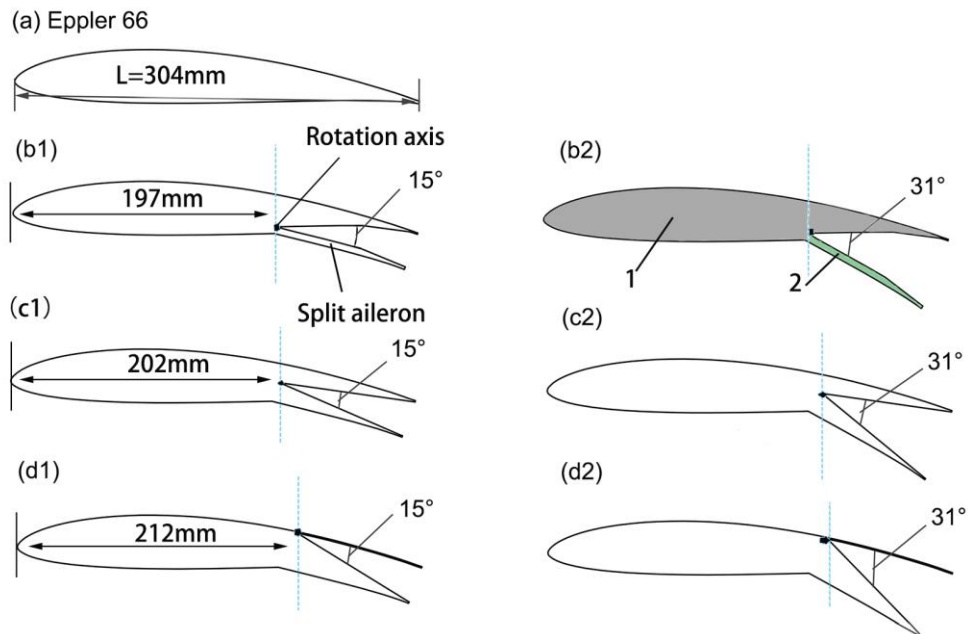
respectively.

Fig. 1. A schematic of the airfoil configuration of the split aileron. (a) Eppler 66, (b) the design model of split aileron at the bottom position, (c) the design model of split aileron at the middle position, and (d) the design model of split aileron at the upper position.

As shown in Fig. 1b-1d, the design of wing consists of two parts: the integrally-smooth upper surface part of wing (sign 1) and split aileron part (sign 2). These two parts constitute the configuration of Eppler 66 when the separated aileron is not deflected. Once the rolling movement of the aircraft needs to be adjusted, the deflection angle of the calm-shell aileron is produced.

2.2 Aerodynamic characteristics of the split aileron

Computational simulations are performed by ANSYS FLUENT software [18] to examine the aerodynamic features of the separated aileron and to visualization display the flow distribution of the surface of the airfoil. Note that, the verification of the independence of computing grid is carried out, which is presented in supplementary materials. The grid of the

computed region around the wing profile is displayed in Fig. 2, the total number of mesh

elements of flow field is about 50800. The far field boundary extends 20L away from airfoil

and the quality of the grid is about 0.8. Wherein the first height of the near wall is about

0.0007m. The far-field boundary conditions are described as follows: V=14 m/s,

ρ =1.225kg/m³, υ =1.7894e-05 kg/(m⊔s), R_e =3×10⁵, and α = -4 ~ 6° at the atmosphere

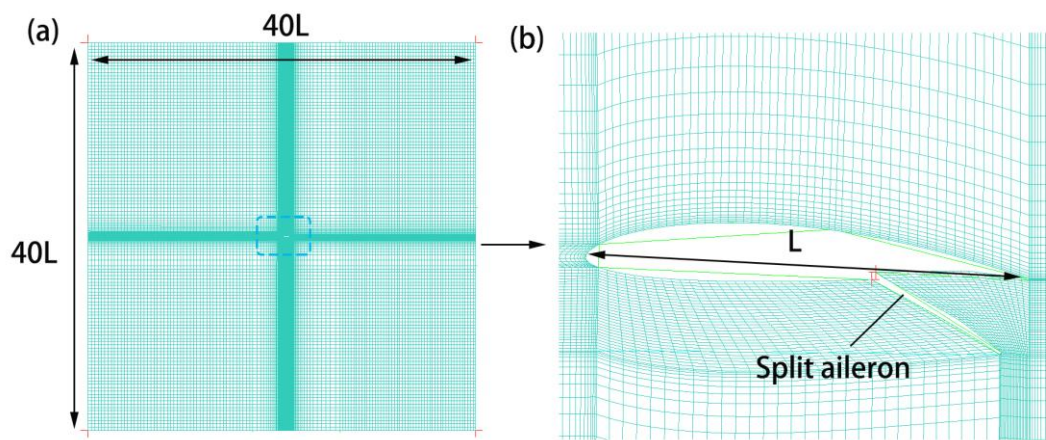temperature of 15 degrees and at the atmospheric pressure of 101325 pa.

Fig. 2. Numerical simulation of 2D airfoil. (a) View of the whole mesh and (b) View of the

near-wall mesh.

The simulation results are represented in Fig 3-5. It is observed that predicted lift

coefficient of Eppler 66 airfoil in Fig. 3. is in accord with numerical results and computational

data available in the literature [19]. In general, the simulation results before stalling are

considered to be believable. As illustrated in Fig. 3-4, compared with three sets of data from

upper, middle and bottom design of the split aileron, the lift and drag coefficient increase with

the increase of the deflection angle of the detached aileron, which is beneficial for improving

aerodynamic performance of the airplane during takeoff and landing to some extent.

Conversely, when the deflection angle become larger than 15°, the result of calculation the

show that the split aileron is detrimental for enhancing the lift-to-drag ratio, as shown in Fig 5.

It can be explained that the increase of the wing camber by changing the deflection angle of the calm-shell aileron, resulting in a growth of both lift and drag and a reduction of the stall speed. Notice that, when the deflection angle of split aileron is equal to 31°, a vortex structure is induced on the lower surface of the wing by the split aileron, which deteriorates the aerodynamics performance of the wing. The detail discussion and visualization vortex structure of the different models of the split aileron are shown in the supplementary material.
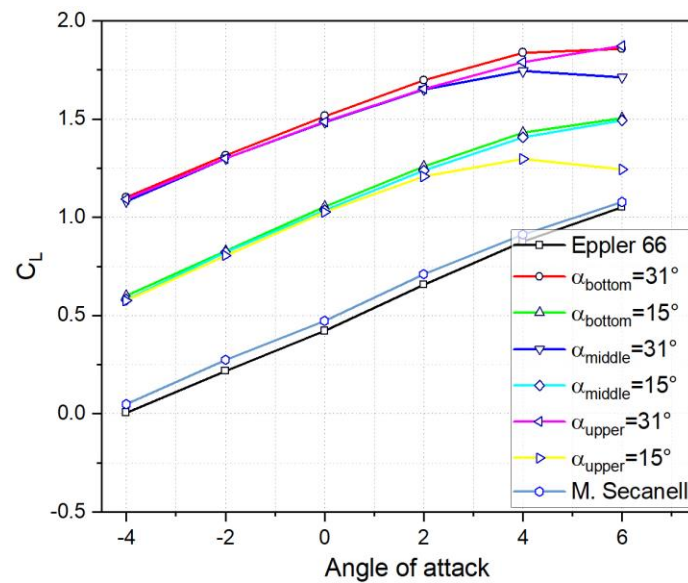
Fig. 3. Effects of split aileron on lift coefficient distribution with different angle of attack.
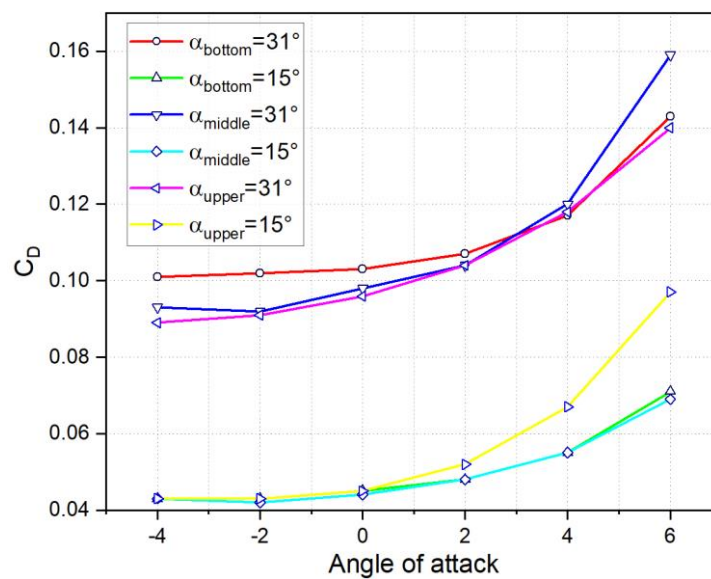
Fig. 4. Effects of split aileron on drag coefficient distribution with different angle of attack.
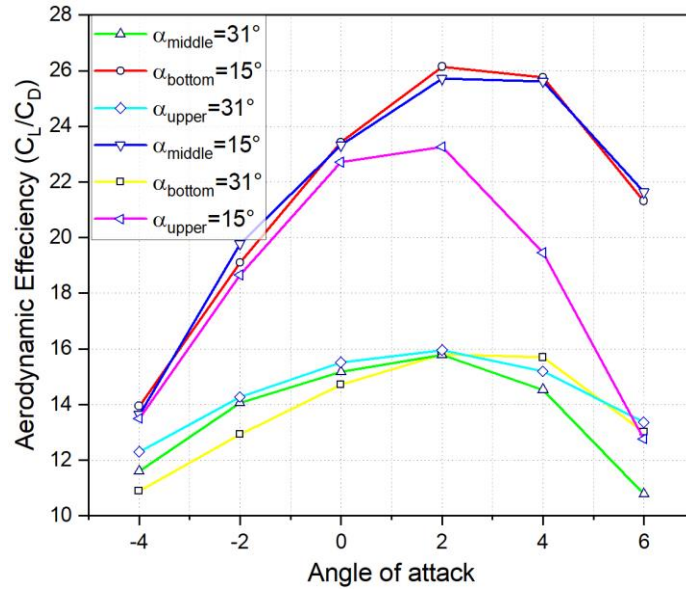
Fig 5. Effects of split aileron on lift-to-drag ratio distribution with different angle of attack.

According to the numerical results, an optimal bottom layout of the design model is acquired. It is noticed that the rudder of deflection angle has an impact on the aerodynamics performance of aircraft wing, which indicates a potential application prospect of controlling the roll movement of aircraft in engineering practice. Therefore, a split aileron can be devised on the under surface of the trailing edge of an aircraft wing, which is used in single to control the aircraft movement around the aircraft's longitudinal axis because of the adequate lift of the wing. In this way, a traditional aileron structure is replaced by a novel design layout of the separated aileron for the fixed wing airplane that is able to comply control in roll motion based on the split aileron deflection. In addition, the design of the bottom split aileron is beneficial to engineering applications, mainly due to for convenience of the processing and installation of structure. Thus, a divided aileron model at the bottom position is manufactured in this study, which is in detail described in Sect. 2.3.

2.3 Split aileron wing design

The design of the wing structural layout with the split aileron of a small fixed-wing UAV

is exhibited in Fig. 6-7, wherein the specific detail parameters are given. It contains twelve

same ribs that are uniform distributed of 126 mm in the wingspan direction to each other. The

main structure of the bearing load is slab, which is located at 55 mm, 150 mm away from the

leading edge of the wing and 77 mm away from the trailing edge of the wing, respectively. In

order to realize a rapid assembly for the wing of the plane, two carbon-fiber rods are mounted

with a distance of 78 mm and 198.5 mm away from the leading edge of the wing. In addition,

a new detached aileron configuration of the wing is devised to act as the control rudder of the

wing with length of 630 mm and width of 90 mm. To present a detail actuator layout of the split

aileron, a closer view is provided in Fig. 7b. A brushless DC motor is installed to provide the
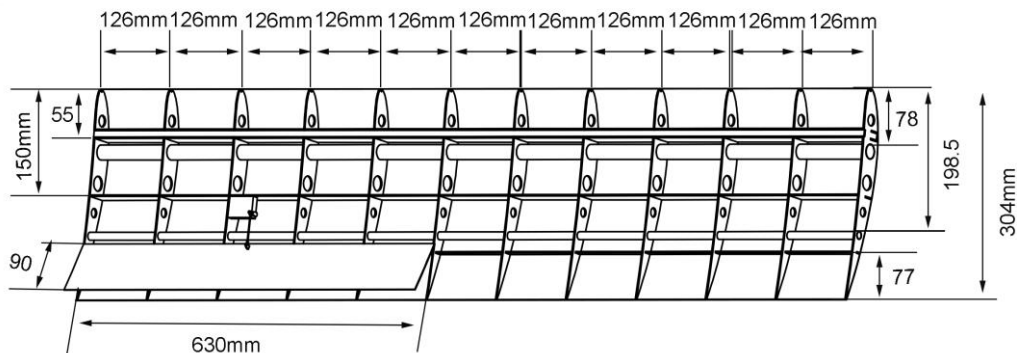
driving force of the split aileron structure.

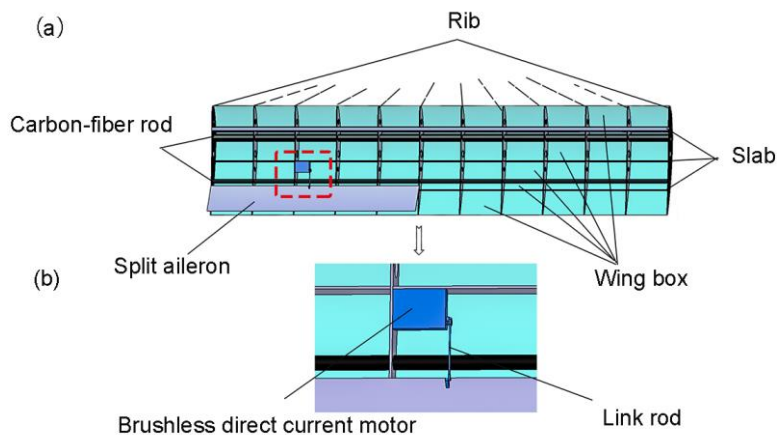Fig. 6. Dimensions of the wing of split aileron.

Fig. 7. The detail wing of the split aileron design.

A prototype of the split aileron wing used in small fixed-wing UAV is developed and assembled in the National key Laboratory of Human Machine and Environment Engineering, as presented in Fig. 8. The servomotor-driven rocker arm system is strategically installed in the middle of the control surface to provide the driving force of the deflection angle of the separate aileron. Note that the rear portion of the lower surface of the wing and the upper surface of immobile wing are closely together to form an integral structure when the separate aileron is located at the initial position. However, once the flight attitude of the rolling of the aircraft need to be changed, the deflection degree of the separated aileron rotates downwards actuated by servomotor-rocker actuating system to produce the rolling moment.
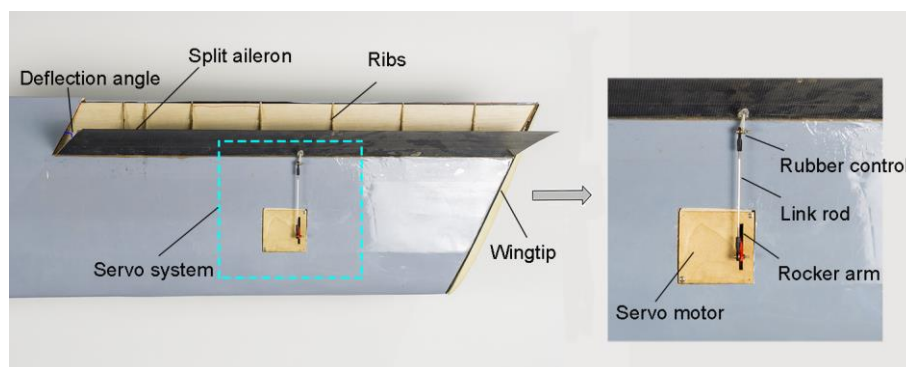

Fig. 8. Bottom view of the manufactured wing model with trailing edge of split aileron.

Fig. 9. Side view of the wing with a newly devised split aileron.

It is apparent that the design of the split aileron implements a smooth surface of the wing indicating that it completely eliminates the assembly gap for the upper surface of the wing, as

illustrated in Fig. 9. In addition, according to the current design, the divided aileron is limited to a single-direction deflection with a deflection of 0 to 31 degrees downward in flight, which is less than the conventional hinged aileron. Herein, the total outboard aileron deflection is about 30 degrees up and 15 degrees down for the general fixed-wing aircraft [20, 21]. Furthermore, compared with traditional hinged aileron in the structure, there is a notable feature that the divided aileron is located on the lower surface of the trailing edge of the wing. When the rotation angle of split aileron is adjusted to 90 degrees, it is treated as a spoiler, which is beneficial to enhance the lading performance of the airplane.

3. Split aileron design analysis

3.1 Aerodynamics performance of the split aileron wing

The aerodynamics feature comparison of the split aileron wing is investigated by a quantitative numerical simulation. Here a wing with a split aileron, a wing with a conventional hinged aileron, and a rectangular NACA0012 wing demonstrator with a chord c=1m and a span L=1m is considered, as described in Fig. 10. In order to exhibit the distinguish of the model design, both ailerons of the wing are deflected at the same position ($\alpha = 15^0$). The portion of the trailing edge aileron is set to be 50% of span and 25% of the chord from the wingtip. The same proportions are applied for the wing of the split aileron and traditional wing of the hinged aileron, where all gaps have a width of 1% of the span.
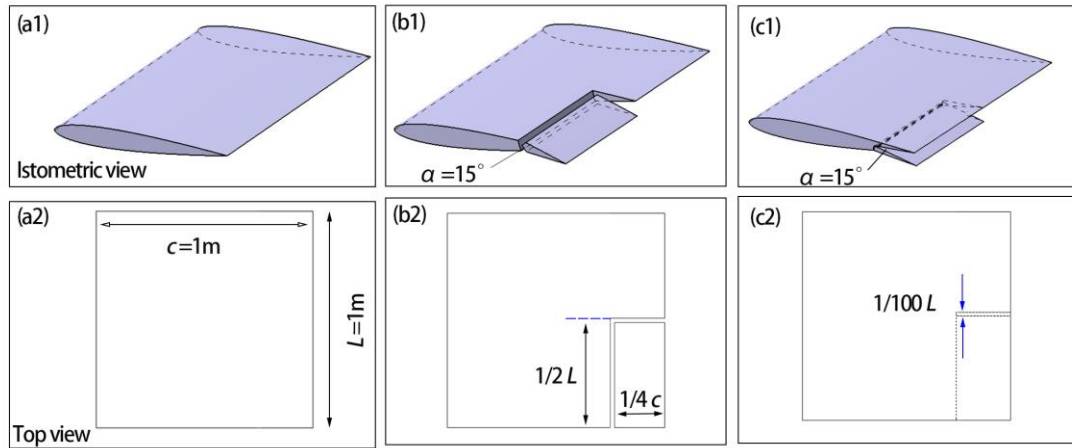
Fig.10. Three models of the wing. (a) a rectangular NACA0012 wing, (b) a wing with conventional hinged aileron, and (c) a wing with a split aileron.

To ensure the reliability of the results, the grid independence test has been made in the present work. Four types of mesh are adopted to examine lift and drag coefficient for NACA 0012 wing with angle of attack 4°, as illustrated in Fig. 10a. The computing results are shown in Table 1, which indicate that the differences of the lift and drag coefficient is within 4% between types 2 and 3. With further increase of grid cell density, the difference can be reduced to less than 3%. Therefore, to implement a relatively high resolution of the grid, the grid density of type 2 is chosen in this work.

Table 1. Mesh independence of NACA 0012 wing at Re=620000 and angle of attack of 4°

Case	Number of cells	Angle of attack 4 °	
		C_L	C_d
1	2000000	0.416	0.00689
2	2850000	0.432	0.00788
3	3550000	0.425	0.00798
4	4250000	0.432	0.008775

It should be noted that the aerodynamic efficiency of the three cases are discussed (NACA 0012 wing, wing with a hinged aileron at $\alpha = 0^0$, wing with a split aileron at $\alpha = 0^0$). A C-type structured grid is adopted in the ICEM CFD software to discretize the flow field around the wing, as presented in Fig. 11. The total number of mesh elements is 2.85 billion, the height of the first layer near the wing wall is 0.000385mm, and the far-field boundary dimension is shown in Fig.11. The far-field boundary conditions are set as follows, Ma=0.115, $Re=0.62 \times 10^6$, a range of angle of attack from $4 \sim 8^0$, and velocity inlet for far-field hold constant for the steady analysis.
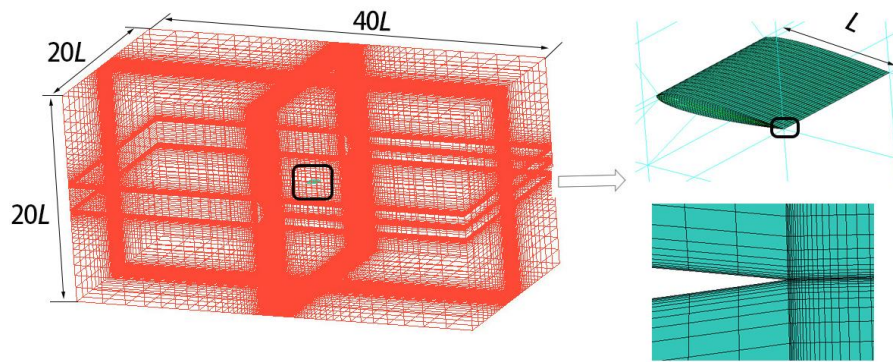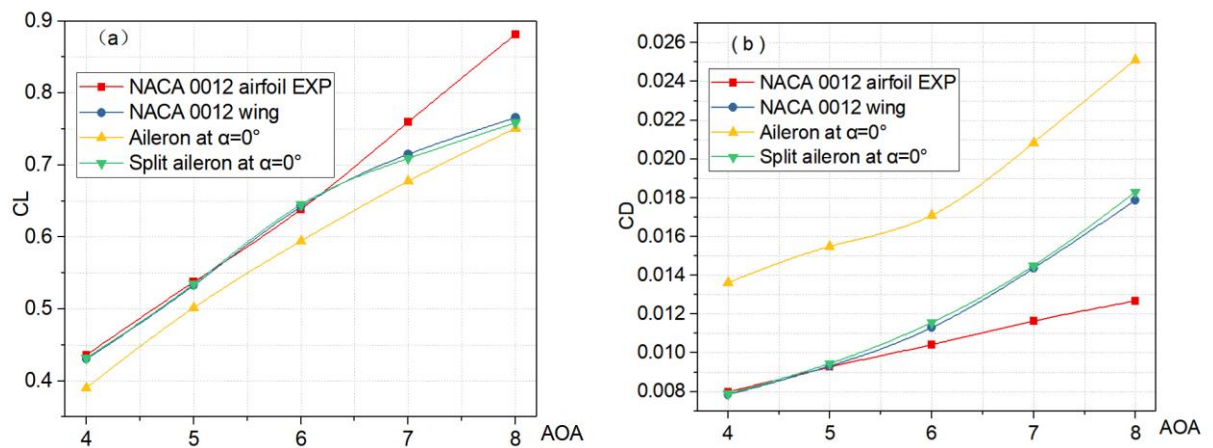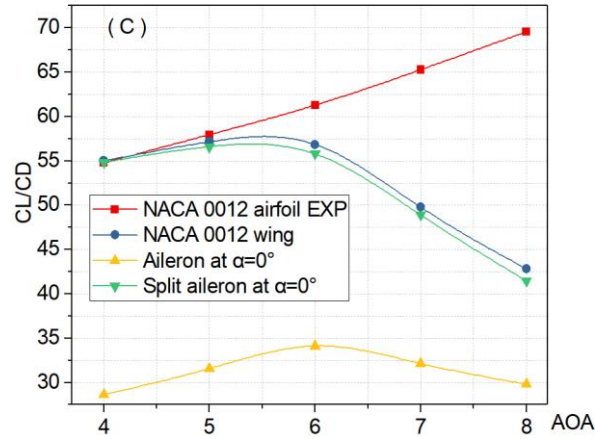

Fig. 11. View of computational domain grid.

Fig. 12. Aerodynamics of the NACA 0012 wing, aileron at $\alpha = 0^0$, and split aileron $\alpha = 0^0$.

(a) lift coefficient as a function of AOA, (B) drag coefficient as a function of AOA, and (c)

lift-to-drag ratio as a function of AOA.

The numerical results are shown in Fig. 12, which indicate that the baseline NACA0012 wing [22] compare well with the experimental results [23], especially in the linear region ($AOA < 6^0$). Note that, the computed results deviate from the experimental data when the angle of attack is larger than 6^0, which might be caused by flow separation. The wing with a split aileron at $\alpha = 0^0$ displays a similar behavior compared with the NACA 0012 wing. However, the wing with the hinged aileron at $\alpha = 0^0$ consistently produces higher drag and lower lift compared with a wing design of the split aileron. It is illustrated that due to the existence of the side-edge gaps cause a reduce of a total wing's effective lift area. Moreover, the total pressure difference is decreased because of the presence of the 1% gaps, which induces pressure loss at the suction side of trailing edge of wing. Compared with the numerical results, a conclusion is capable of being drawn: the wing with a split aileron can enhance the average lift and characteristic efficiency by 6.02 % and 16.3 %, respectively, and the drag is reduced by 34.2%.

3.2 Weight analysis of the split aileron

The material adopted of the novel split aileron is identical to those ailerons of the traditional fixed-wing airplane, which involves 3k carbon fabric ($\rho = 220 \text{g/m}^3$), polymethacrylimide (PMI) foam ($\rho = 45 \text{kg/m}^3$), and 40 percent of filling glue, as depicted in Fig. 13-14. Furthermore, to compare the total weight of the two types of designed structures, the fabrication technology and method of the split aileron and the conventional aileron are utilized in the same way. However, it should be noted that there are particular features of the configuration of the split aileron. It includes the geometry dimension of aileron model and the position of PMI foam padded in the structure.
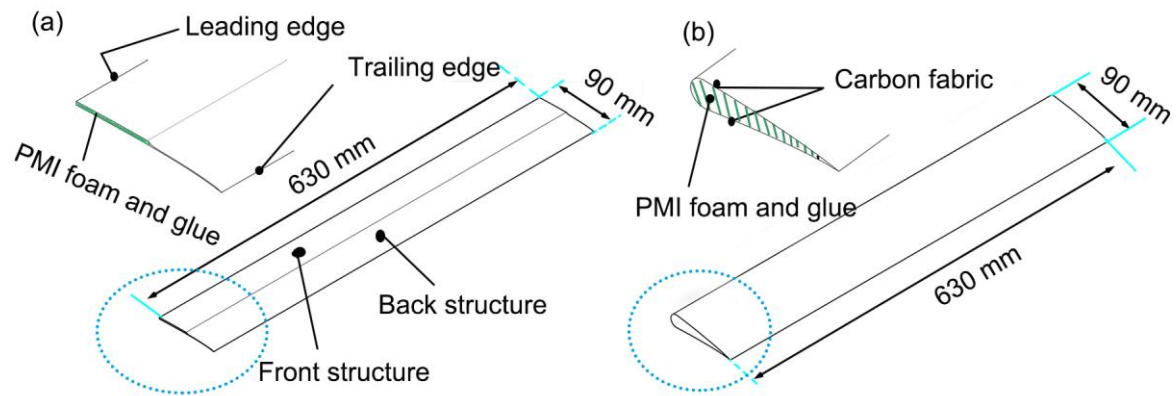
Fig. 13. The geometry dimension and material component of the model. (a) split aileron structure, (b) traditional hinged aileron structure.
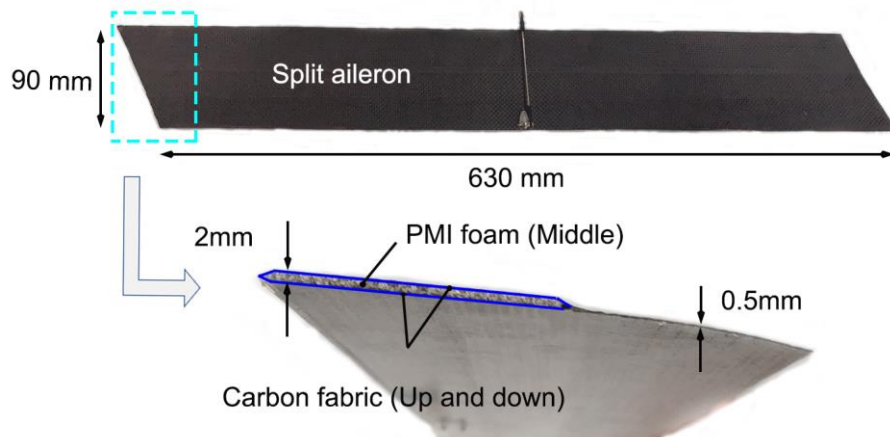
Fig. 14. The fabricated structure model of the split aileron.

The geometry sizes of the split aileron in the front and rear half structures are 63 mm x 9 mm x 2 mm, 63 mm x 9 mm x 0.5 mm, respectively, as provided in Fig. 13a and 14. It can be observed that the PMI foam-core sandwich is not filled on the trailing edge of the detached aileron, and the main reason is to maintain the shape of the airfoil due to the thin feature of the trailing edge of wing. In contrast, the configuration of the conventional hinged aileron is an integrated shape of airfoil without a sudden transition. The perimeter and volume of the traditional aileron model are 200 mm and 863 mm^6 in the case of the equal dimensions of length and width. Moreover, in order to assure a safe structure of the aileron, the entire inner space of the aileron is padded with the PMI foam.

Table 2. Comparison of single-aileron weight value obtained from the split aileron and the traditional hinged aileron.

Component	Parameters		Mass	
	Split aileron	Conventional aileron	Split aileron	Conventional aileron
Carbon fabric	0.1134 m^2	0.126 m^2	24.9 g	27.7 g
PMI foam	$4.25 \times 10^{-5} m^2$	8.63×10^{-4} m^2	1.19 g	24.5 g
Filled glue	40% glue	40% glue	17.9 g	53.3 g

A quantitative comparison is demonstrated in Table 2, where it lists the weights of different compositions of a single aileron acquired from the model of the separated aileron and conventional hinged aileron in the present model. The overall weight on each side is 58.2 g and 105.5 g for the split aileron and common aileron of aircraft. It is concluded that the design of the divided aileron can reduce weight by up to 52.2 g.

4. Prototype development and flight test

4.1 Prototype development of the split aileron wing

The three installation positions of the split aileron are proposed, as displayed in Fig.1. Based on the aerodynamic analysis for the three design schemes, an optimal location of the bottom of the detached aileron structure is determined, which not only implements better aerodynamics performance but also motivates a potential practical application for small fixed-wing airplane. The wing structure is manufactured from light balsa wood and glue-laminated wooden, with thickness of 1 mm, 2mm and 3 mm, respectively. It should be noted that the split aileron structure is made of carbon fibers, PMI foam, and 40% of glue for lighter weight and higher strength and rigidity, as described in Sect. 3.2.

Fig. 15. The test plane of the split aileron wing.

In order to verify the innovative design scheme of the wing with split aileron, an electric prototype model is fabricated with take-off weight of 8 kilograms, which is less than the maximum takeoff weight design of 9 kilograms of the aircraft, as shown in Fig. 15. There are special features for the design of the fixed-wing aircraft. It includes a conceptual design of joined-wing configuration that is employed to expand the wing area and acquire a good stability of aircraft. To mount the wings to the fuselage, the front and rear of the wings are

installed by the 20 mm×18 mm and 10 mm×8 mm carbon fiber rod, respectively. Then, the connection of the front and rear of the wing is assembled through fours M6×25 mm nylon screws at the left and right support structure.

4.2 Flight test

To examine the validity of the numerical results and verify the reliability of the structure design scheme of the split aileron, the flight test is carried out by a remote controller (FUTABA 16sz) in a region of space. There are some essential preparations on ground before the flight test as follows. (1) The flight attitude of rolling and pitching is calibrated such that the resolving of the flight control system is ensured precisely. (2) A standardized test is applied to the airspeed measuring sensor to display exactly and avoid flight safety of the plane. (3) The function tests of the control surface are firstly conducted on the developed aircraft. Then, flight test is compiled by the flight operator of the aircraft who can remotely adjust the deflection angle of the split aileron and rudder and elevator of the rear wing via the ratio control.

Fig. 16. The fight test of the plane with split aileron.

Fig. 16 illustrates a camera shot of the flying aircraft in flight, which is presented in detail

in the supporting material. It is explicit that if a pilot tries to maneuver with the rudder alone, the side-slip angle of the aircraft will be induced by centrifugal force. However, the aircraft turns smoothly in fight reveals that the pilot attempts to adjust the heading by rudder and split aileron. Moreover, it is also demonstrated that the proposed design of the servo drive system is manipulated reliably, and the separated aileron structure is able to endure the aerodynamic forces. Therefore, it is confirmed that a novel wing configuration with split aileron is apt and credible based on the results of flight test, which is promising in small fixed-wing UAV for future engineering applications.

5. Conclusions

In the current work, an innovative structure design of the split aileron for fixed-wing aircraft is proposed, which is capable of realizing the function of a conventional hinged aileron. The detached aileron not only is able to control the roll motion of a small airplane in flight based on the aerodynamic forces, but also obtain no innate assembled gap of the wing on the upper surface during the heading modification process. In order to acquire an optimal installation position of the split aileron, three types of design models, i. e., the upper, middle and lower models are elected. The aerodynamic characteristics and structural weight of the divided aileron are assessed by comparison with a conventional hinged aileron. To verify the validity of the numerical results and the rationality of the structural design, a functional prototype of the split aileron-wing equipped fixed-wing UAV is fabricated and assembled based on the independent design.

The numerical results of three models indicate that the optimal bottom configuration of the design model is acquired by the analysis of the three kinds of split aileron. In addition, a

conclusion can be drawn that the wing with a split aileron can enhance the average lift and aerodynamic efficiency by 6.02 % and 16.3 %, respectively, and the drag is reduced by 34.2%. The weight of split aileron is only 55.2% of the conventional hinged aileron. Finally, the flight test results confirm that the split aileron is credibly and stably controlled for the rolling motion of aircraft, which is potential promising for future engineering application.

Further work will be focused on the wind tunnel test and 3D model analysis for a real fixed-wing plane, especially for a general vertical takeoff and landing (VTOL) solar powered airplane. The smoothness of the upper surface of the wing will increase the laying area of the solar cell based on the design scheme of the split aileron.

Conflict of interest statement

There is no conflict of interest.

References

[1] F. Centracchio, M. Rossetti, U. Iemma, Approach to the Weight Estimation in the Conceptual Design of Hybrid-Electric-Powered Unconventional Regional Aircraft, Journal of Advanced Transportation, DOI 10.1155/2018/6320197(2018).

[2] V. Grewe, L. Bock, U. Burkhardt, K. Dahlmann, K. Gierens, L. Huettenhofer, S. Unterstrasser, A.G. Rao, A. Bhat, F. Yin, T.G. Reichel, O. Paschereit, Y. Levy, Assessing the

climate impact of the AHEAD multi-fuel blended wing body, Meteorologische Zeitschrift, 26 (2017) 711-725.

[3] P. Okonkwo, H. Smith, Review of evolving trends in blended wing body aircraft design, Progress in Aerospace Sciences, 82 (2016) 1-23.

[4] R. Kirner, L. Raffaelli, A. Rolt, P. Laskaridis, G. Doulgeris, R. Singh, An assessment of distributed propulsion: Part B - Advanced propulsion system architectures for blended wing body aircraft configurations, Aerosp. Sci. Technol., 50 (2016) 212-219.

[5] C. Huijts, M. Voskuijl, The impact of control allocation on trim drag of blended wing body aircraft, Aerospace Science & Technology, 46 (2015) 72-81.

[6] L.L. Gamble, D.J. Inman, A tale of two tails: Developing an avian inspired morphing actuator for yaw control and stability, Bioinspiration & Biomimetics, 13 (2018).

[7] F. Mohamad, W. Wisnoe, R. Nasir, W. Kuntjoro, A Study about the Split Drag Flaps Deflections to Directional Motion of UiTM's Blended Wing Body Aircraft Based on Computational Fluid Dynamics Simulation, 2012.

[8] N.U. Rahman, J.F. Whidborne, Propulsion and Flight Controls Integration for a Blended Wing Body Transport Aircraft, J. Aircr., 47 (2009) 895-903.

[9] F. Mohamad, W. Wirachman, W. Kuntjoro, R.E.M. Nasir, The Effects of Split Drag Flaps on Directional Motion of UiTM's BWB UAV Baseline-II E-4: Investigation Based on CFD Approach, Advanced Materials Research, 433-440 (2012) 584-588.

[10] G. Stenfelt, U. Ringertz, Yaw Control of a Tailless Aircraft Configuration, J. Aircr., 47 (2010) 1807-1810.

[11] N. Molin, D. Angland, Z. Xin, L.C. Chow, Measurements of Flow Around a Split Flap

Configuration, Aiaa Aerospace Sciences Meeting & Exhibit, 2007.

[12] Y. Pan, J. Huang, Research on lateral-directional stability augmentation system of flying wing aircraft based on reliability model, Proceedings of the Institution of Mechanical Engineers, Part G: Journal of Aerospace Engineering, 5 (2018) 0954410018817449.

[13] X. Qu, W. Zhang, J. Shi, Y. Lyu, A Novel Yaw Control Method for Flying-wing Aircraft in Low Speed Regime, Aerospace Science & Technology, 69 (2017).

[14] P. Mardanpour, D.H. Hodges, Passive morphing of flying wing aircraft: Z-shaped configuration, J. Fluids Struct., 44 (2014) 17-30.

[15] Z. Jian Li, D. Li Ma, Control Characteristics Analysis of Split-Drag-Rudder, 2014.

[16] D. Li, Q. Liu, Y. Wu, J. Xiang, Design and analysis of a morphing drag rudder on the aerodynamics, structural deformation, and the required actuating moment, Journal of Intelligent Material Systems and Structures, 29 (2018) 1038-1049.

[17] J. Rajput, W.G. Zhang, X.B. Qu, A Differential Configuration of Split Drag-Rudders with Variable Bias for Directional Control of Flying-Wing, Applied Mechanics and Materials, DOI (2014).

[18] A. Fluent, ANSYS FLUENT 14.5 Theory Guide, DOI (2012).

[19] M. Secanell, A. Suleman, P. Gamboa, Design of a Morphing Airfoil Using Aerodynamic Shape Optimization, Aiaa J., 44 (2006) 1550-1562.

[20] Boeing, Aircraft Maintenance Manual (AMM) Supplement, DOI (2014).

[21] I.H. Abbott, A.E. Von Doenhoff, Theory of Wing Sections, General Information, DOI (1959).

[22] R.E. Sheldahl, P.C. Klimas, Aerodynamic characteristics of seven symmetrical airfoil

sections through 180-degree angle of attack for use in aerodynamic analysis of vertical axis wind turbines, ; Sandia National Labs., Albuquerque, NM (USA), 1981, pp. Medium: ED; Size: Pages: 120.

[23] C. Abdessemed, Y. Yao, A. Bouferrouk, P. Narayan, Analysis of a 3D Unsteady Morphing Wing with Seamless Side-edge Transition, 2018 Applied Aerodynamics Conference2018.